



Molecular clocks without rocks: new solutions for old problems

George P. Tiley¹, Jelmer W. Poelstra¹, Mario dos Reis², Ziheng Yang³, Anne D. Yoder^{1,*}

¹Department of Biology, Duke University, Durham, NC 27708, USA

²School of Biological and Chemical Sciences, Queen Mary University of London, London E1

4NS, UK

³Department of Genetics, Evolution, and Environment, University College London, London

WC1E 6BT, UK

*Correspondence: anne.yoder@duke.edu

Keywords: Divergence Time Estimation, Multispecies Coalescent, Substitution Rate, Mutation Rate, Effective Population Size, Gene Tree Discordance

Abstract

Molecular data have been used to date species divergences ever since they were described as "documents of evolutionary history" in the 1960s. Yet, an inadequate fossil record and discordance between gene trees and species trees are persistently problematic. We examine how, by accommodating gene tree discordance and by scaling branch lengths to absolute time using mutation rate and generation time, multispecies coalescent (MSC) methods can potentially overcome these challenges. We find that time estimates can differ — in some cases, substantially — depending on whether MSC methods or traditional phylogenetic methods that apply concatenation are used, and whether the tree is calibrated with pedigree-based mutation rates or with fossils. We discuss the advantages and shortcomings of both approaches and provide practical guidance for data analysis when using these methods.

27 **Divergence Time Estimation**

28 Zuckerkandl and Pauling [1] were the first to posit that genetic distances between organisms
29 could be converted to absolute geological times, describing genomes as "documents of
30 evolutionary history." The most commonly used **molecular clock** methods (See Glossary)
31 estimate absolute times from genetic distances by calibrating the **species tree** with fossil data,
32 assuming either a constant rate of evolution among lineages (the molecular clock) or variable
33 rates (**relaxed clock models**) [2-4]). Recently, the **multispecies coalescent (MSC)** [5] is on
34 the ascent as a method for estimating divergence times [6, 7] due at least in part to potential
35 freedom from **fossil calibrations** [8, 9]. However, conflicts can arise in empirical studies
36 between **traditional phylogenetic clock models** and MSC methods, raising the question of
37 which method is more reliable for placing evolutionary events in a temporal context. Here, we
38 examine the fundamental assumptions and analytical details of these two general
39 methodological classes: 1) Traditional phylogenetic clock models that use **concatenation** of
40 genetic **loci** and 2) MSC models that explicitly model **gene tree discordance** due to
41 **incomplete lineage sorting (ILS)**. Both approaches can be used without fossil calibrations
42 where *a priori* information on absolute rates of evolution are available, but some features of the
43 MSC are ideal for estimating species divergence times by leveraging external **de novo**
44 **mutation rate (μ)** estimates, typically measured from pedigree trios (Fig. 1; Key Figure). We
45 conclude by describing conditions that influence the suitability of the two approaches and offer
46 recommendations for the proper application of both.

47

48 **The Allure of the Molecular Clock**

49 Clock models and their applications have had enormous impacts on our understanding of the
50 history of life on earth, including the timing of life history transitions [10], global ecological
51 change in response to climate oscillations [11], the ancient origins of orders such as
52 Lepidoptera [12], and even the origin of life or the last universal common ancestor (LUCA) after

53 the Moon-forming impact [13]. Calibration of the molecular clock has historically been
54 performed using fossil ages [14] or geological events [15] though only a tiny fraction of
55 phylogenetic lineages have reliable fossil records for appropriate calibration [16]. Thus, the lack
56 of a detailed fossil record for many groups is a major constraint for investigating the evolutionary
57 history of those lineages. For instance, both plant [17] and animal fossils [18] are difficult to
58 characterize in tropical rainforests where available rock formations for fossilization are typically
59 absent [19]. In some groups, such as grasses, calibrations based on phytolith microfossils are
60 contentious because of ambiguous diagnostic characters that compromise accurate
61 phylogenetic placement [20]. And for many groups, such as the glass frogs [21], fossils are
62 entirely absent.

63

64 Thus, for the analysis of most clades across the tree of life, investigators must depend on fossil
65 calibrations that are phylogenetically distant from the organisms of interest. As phylogenetic
66 distance increases, the complexities of modeling rate variation among lineages also increases
67 given the now extensive evidence that molecular rates change frequently across phylogeny.
68 Finally, a growing body of literature suggests that by ignoring genetic polymorphism in ancestral
69 species, divergence times may be systematically biased [6, 7, 9].

70

71 **Relaxed Clock Models**

72 When a calibration point can be placed with confidence within a given clade and close to its
73 **most recent common ancestor (MRCA)**, it is possible to estimate **per-year substitution**
74 **rates**. Using that rate, an investigator can then infer divergence times for other nodes in the
75 phylogeny that do not have fossil calibrations. This assumes, however, that all lineages share a
76 single rate of evolution: i.e., that there is a **strict molecular clock**. While this is not an
77 unreasonable assumption for closely related species, the strict clock is typically violated when
78 more distantly related species are included [22]. Such violations can arise not only from

79 differences in the molecular mechanisms that generate mutations [23], but also from variation in
80 life history traits [24, 25]. For example, great apes have lower substitution rates compared to
81 Old World and New World monkeys (the hominoid slowdown hypothesis [26]), a phenomenon
82 that can largely be explained by differences in **generation time** among species [27]. Similar
83 observations have been made in plants by comparing woody and herbaceous species [28, 29].
84
85 The clock can be "relaxed" by allowing for variable rates among branches on a phylogeny while
86 maintaining computational tractability and statistical identifiability [2, 3, 30, 31]. The first relaxed
87 clock methods that could leverage uncertainty across multiple calibrations were implemented
88 with maximum likelihood and required *a priori* assumptions to partition branches into different
89 rate groups (e.g., "local clocks" [32] or heuristic approaches [33, 34]). Recent **Bayesian**
90 **methods** have incorporated uncertainty in calibrations and as well as in rates of evolution
91 through the use of **prior distributions**. Different models of rate variation among branches are
92 available, including autocorrelation among lineages [2, 35], uncorrelated rates [3, 30, 36], or a
93 mixture of the two [37]. However, per-year substitution rates and divergence times are sensitive
94 to prior distribution on node calibrations [38] and justifying informed node calibrations is not
95 trivial [39]. Relaxed clock methods have recently been extended to account for uncertainty in
96 fossil placement [40] by leveraging morphological data from both extant and fossil species [41-
97 44]. These **total-evidence** [41] approaches include **tip-dating methods** that treat extinct fossil
98 lineages as tips where fossil occurrence [40] or morphological characters from fossils [43] can
99 calibrate rates of evolution to absolute time. They can also incorporate different speciation
100 mechanisms that best suit an organismal group [45]. As with more traditional methods,
101 however, these total-evidence tip-dating methods can only be applied to clades with an
102 available fossil record [42] and therefore cannot solve the problem of poor or absent fossil
103 records.

104

105 Tip-dating methods that use only molecular data [46, 47] offer one approach for overcoming an
106 absence of fossil calibrations. These methods have been applied to viruses, where high
107 substitution rates generate sufficient variation from contemporary samples to determine relative
108 ages [48], as well as to cases wherein ancient DNA samples can calibrate the molecular clock
109 such as for woolly mammoths [49] and humans [50]. Even so, **ancient DNA methods** are
110 equally or even more restrictive than fossil-calibrated methods given that they can only be
111 applied to a limited number of organisms for which well-preserved and relatively recent samples
112 are available [51]. Most significantly, all of the above methods use **concatenation** of genetic
113 loci, thereby making the fundamental assumption that the phylogenetic history of each locus
114 matches the species tree. We here discuss how concatenation can be problematic, and how
115 MSC methods overcome these problems.

116

117 **The Multispecies Coalescent as a Backward Time Machine**

118 **Coalescent** theory is a branch of population genetics that describes the genealogical histories
119 of a sample of alleles in a population, going back from a sample of extant alleles to their most
120 recent common ancestor [52]. Two alleles are said to coalesce when they share a common
121 ancestor. The MSC is a simple extension of the single-population coalescent to multiple species
122 [5] and accommodates the species phylogeny and the coalescent processes in both the extant
123 and extinct species [53, 54]. The MSC jointly estimates **divergence times** and rates of
124 evolution (Fig. 1) while explicitly modeling gene tree discordance due to incomplete lineage
125 sorting (ILS, also known as deep coalescence). ILS occurs when sequences from different
126 species fail to coalesce in their most recent ancestral species. The shorter the branch in
127 coalescent units between two speciation events, the more likely is ILS to occur (Box 1). Short
128 coalescent branch lengths can be caused not only by small time intervals between speciation
129 events, but also by large ancestral **effective population size**.

130

131 It is now well accepted that gene trees do not consistently match species trees [55]. Though this
132 was initially considered to be a hindrance to the accurate reconstruction of phylogenies [56],
133 investigators are increasingly aware that these heterogeneities provide valuable information
134 about the timing and population dynamics of organismal lineages over their evolutionary history.
135 Described as a "backward time machine" [57], the MSC treats the stochastic variation of the
136 coalescent process over genes or genomic regions as a source of information rather than as
137 "mistakes" or "conflicts", and is thus uniquely suited to harness the power of many loci from
138 modern genomic data. Accordingly, the MSC is of increasing interest to investigators who seek
139 to place divergence events in a temporal context. The MSC makes a number of simplifying
140 assumptions including a lack of post-divergence **gene flow**, ILS as the only source of gene tree
141 discordance, no recombination within loci, and a lack of selection. Where high amounts of gene
142 flow among non-sister species are a concern, extensions to the MSC are available [58].

143

144 **Accounting for the Coalescent Process**

145 Traditional phylogenetic clock models equate species divergence (i.e., "split times") to sequence
146 divergence. This is problematic given that sequence divergence will always predate speciation
147 events in the absence of gene flow [59, 60] (Fig. 2). In contrast, coalescent methods explicitly
148 accommodate the differences between the two and directly estimate *species* divergence times
149 which are generally the evolutionary events of interest (Fig. 3; Box 2). Moreover, when fossil
150 calibrations are used, divergence time estimates can be strongly affected, with the direction of
151 the bias depending on the placement of the most precise calibrations. If these calibrations are
152 placed on young nodes within a phylogeny, divergence times will be underestimated across the
153 entire phylogeny, while if calibrations are placed on ancient nodes, the ages of young nodes are
154 likely to be overestimated. Accordingly, for phylogenies with complex mixtures of fossil
155 calibrations, both underestimation and overestimation of divergence times may occur across the
156 phylogeny – regardless of the analytic method applied.

157
158 Traditional phylogenetic analysis of concatenated sequences assumes that a single tree
159 topology with one set of divergence times underlies the multilocus sequence data, irrespective
160 of how rate variation is modeled among sites, loci, or branches. Gene tree discordance due to
161 ILS then appears as additional substitutions on branches in the species phylogeny [6, 61],
162 leading to overestimation of species divergence times when ILS is not accounted for [9]. In line
163 with these theoretical expectations, Stange et al. [7] showed that in cases of high gene tree
164 discordance, concatenation methods will overestimate ages of young nodes when ancient
165 nodes are constrained. Similarly, Fang et al. [62] found that recent species divergences were
166 correctly estimated to be more recent when using MSC methods. Simulations generally suggest
167 that the MSC can improve divergence time estimates when gene tree discordance is high [7, 9],
168 while comparable performance should be expected between concatenation and MSC methods
169 when gene tree discordance is low (Fig. 3).

170
171 Although empirical studies using MSC approaches have thus far focused on recent species
172 divergences (1-10 MYA) [7, 62, 63], the effects of discordant gene trees should also impact
173 divergence time estimates for older divergences where the coalescent branch length is short
174 and ILS is high [9]. These patterns are expected for rapid radiations that occurred deep in
175 evolutionary history, such as placental mammals [64], passerine birds [65], and lepidopterans
176 [12]. Divergence time estimates for these groups are important for interpreting species
177 biogeography and trait evolution, and as computational efficiency and resources continue to
178 improve, the evolutionary history of these groups should be re-evaluated with MSC models that
179 also leverage fossil calibrations. In angiosperms, reconciliation of molecular dates with those
180 interpreted from the fossil record has been the topic of vigorous debate even though molecular
181 data have largely been restricted to chloroplast sequences, which represent a single **gene tree**

182 [66-69]. As large multilocus nuclear datasets become increasingly available for plants [70], the
183 benefits of fossil-calibrated MSC methods could be realized.

184

185 **The Coalescent Time Unit**

186 Because the average coalescence time between two randomly sampled sequences from a
187 diploid population is $2N$ generations, it is convenient to scale branch lengths in the species tree
188 in coalescent units, that is, to use $T = t/(2N)$ where t is the number of generations until the
189 coalescent event. T can also be rescaled by mutations and represented as $\tau = \mu t$, where μ is the
190 per-generation mutation rate, so that $T = \tau/(\theta/2)$. Here $\theta = 4N\mu$ is the population-scaled
191 mutation rate; a fundamental parameter in population genetic models which represents the
192 average number of mutations per site between two sequences randomly sampled from the
193 population.

194

195 MSC programs like StarBEAST2 [6] and BPP [5, 71] use multilocus sequence alignments to
196 estimate species trees as well as parameters in the MSC model including species divergence
197 times (τ) and population sizes (BPP estimates θ and StarBEAST2 estimates $N\mu$), both
198 measured by the expected number of mutations per site. If fossil calibrations or mutation rates
199 are available to calibrate the tree, they can be used to convert genetic distance to absolute
200 times and absolute rates. When a per-generation mutation rate is available, generation times
201 are also necessary (Fig. 1) to convert to divergence times in years. This approach assumes that
202 the per-generation mutation rate and generation time are constant throughout the species tree,
203 which is a reasonable assumption for analyses of closely related species for which genetic
204 divergences likely satisfy a strict clock [72, 73].

205

206 ***de novo* Mutation Rate Estimates Provide Freedom from the Fossil Record**

207 In order to estimate absolute divergence times in the absence of fossil calibrations, direct
208 estimates of the mutation rate estimates are needed. Recently, whole-genome sequencing data
209 from **pedigree trios** have been used to estimate the **de novo mutation rate** for many animals
210 [74-78] and parent-progeny pairs in plants [79]. Recent examples of divergence time estimation
211 based on mutation rates and **coalescent age estimates** include the age of human migration
212 events [80] and of domestication histories among agriculturally important species [81-83].

213

214 To estimate a *de novo* mutation rate, the father, mother, and offspring from a pedigree trio are
215 sequenced and aligned to a reference genome. Variants detected in the child that are distinct
216 from both the mother and father and do not match the reference are considered *de novo*
217 mutations. Because the number of sequencing errors are more than an order of magnitude
218 greater than the number of true mutations, strict filtering criteria in computational analysis must
219 be applied to the called variants to avoid false positives. Also, mutations cannot be identified at
220 all sites because of variable sequencing read depth and alignment uncertainty in repetitive
221 regions. Thus, the number of **callable sites** needs to be estimated as the denominator to
222 accurately estimate μ [76]. Ideally, the final estimate of μ is averaged over multiple pedigrees,
223 as any single pedigree will yield few mutations. Best practices for reducing false positives and
224 false negatives for inferred mutations are still being developed [84].

225

226 The availability of a reference genome can be a critical limitation for estimating *de novo*
227 mutation rates in non-model organisms. Although high-quality reference genomes are
228 anticipated for most Eukaryotic lineages in the near future [85], there will ultimately be barriers
229 for some groups. In the absence of direct estimates of μ for a species of interest, distributions of
230 μ can be developed based on studies of related organisms [72]. Generation time estimates must
231 be considered as well given that mutation rates from pedigree studies are scaled by generation
232 to recover absolute divergence times (Fig. 1).

233

234 **Discrepancies between Concatenation and MSC methods for Divergence Time Estimates**

235 Though empirical examples are as yet few, discrepancies between divergence dates estimated
236 by fossil-calibrated concatenation and mutation rate-calibrated MSC methods are emerging
237 (e.g., Fig 4). For the closely related species pair of human and chimpanzees, the mutation rate-
238 calibrated MSC [9] and concatenated time estimation give similar results. Fossil-calibrated
239 concatenation and fossil-calibrated MSC methods place the divergence between 5.7 and 10
240 MYA, typically near the center of the calibration density at 7.5 MYA [9, 86]. A mutation rate-
241 calibrated MSC analysis that assumed the human mutation rate for both species recovered a
242 posterior mean of 8.2 MYA [9]. Divergence time estimates calibrated directly with mutation rates
243 but not using the MSC are also similar, but only after considering the difference between
244 species and sequence divergence. In one such study, **pairwise sequence divergence**
245 between chimp and human (t_{Seq} ; Fig. 2) yielded a divergence time of 12.1 MYA assuming the
246 human mutation rate [27], though subtracting $2N_{HC}$ (the effective population size for the human-
247 chimpanzee common ancestor) yields a divergence time of 7.9 MYA. Thus, per-generation
248 mutation rates can be used to estimate divergence times from concatenated data too, but the
249 difference between species divergence and sequence divergence needs to be accommodated
250 by some calculation of population size estimate (Fig. 2).

251

252 The sensitivity of these methods to the mutation rate estimate is keen. For example, when the
253 human mutation rate was applied unilaterally across a primate phylogeny, a divergence time
254 between Old world monkeys (*Macaca mulatta*) and humans of 62 MYA was recovered [87], in
255 stark contrast to the 35 MYA age estimate indicated by fossil evidence [86]. The discrepancy is
256 likely explained by a slower mutation rate in humans compared to Old World monkeys [88] and
257 indicates that caution is needed when applying pedigree-based mutation rates to divergence
258 time estimation, especially across large phylogenies. While one possible reason for

259 discrepancies across long times scales is that purifying selection may lead to lower substitution
260 rates compared to mutation rates [89], as observed in mutation accumulation lines with
261 *Arabidopsis thaliana* [90], the discrepancy in this case was in the opposite direction. Thus, given
262 the small number of empirical examples at present, it is difficult to generalize the causes of
263 disparities between substitution and mutation rates at present.

264

265 In one such empirical example, MSC methods produce significantly more recent age estimates
266 than fossil-calibrated concatenation methods for mouse lemurs (genus *Microcebus*). Whereas a
267 mutation rate-calibrated MSC analysis yields a MRCA for the genus of 1.5 MYA [63], previous
268 analyses using fossil-calibrated concatenation methods yielded estimates of ~10 MYA [86, 91].
269 Though this discrepancy could, in part, be the consequence of a falsely elevated pedigree-
270 based mutation rate estimate [91], the discrepancy would still be pronounced even if the true
271 rate is only half of the estimated rate. Conversely, for the fossil-calibrated divergence time
272 estimate using concatenation, phylogenetically distant, external calibrations [86, 91] were used
273 by necessity given that there is a complete dearth of fossils within the lemuriform clade. As
274 described above, the fossil-calibrated concatenation estimate is thus likely to overestimate
275 divergence times for young nodes given the dependence on older fossil calibrations deeper in
276 the phylogeny (Fig. 3; [9]). This is similar to cases of Stange et al. [7] and Fang et al. [62] where
277 MSC methods using geological calibrations resulted in more recent divergence times compared
278 with those found with concatenation – even when using the same calibrations. In summary, it is
279 important to note that the differences in time estimates between the MSC and phylogenetic
280 concatenation methods may be complex, depending on biases of mutation rate estimates and
281 on the relative placement of calibrations within the phylogeny.

282

283 **A New Frontier in Divergence Time Estimation**

284 Divergence time estimates can fundamentally affect interpretations of trait evolution,
285 biogeography, and the processes that underlie species radiations. Thus, the stakes for
286 evolutionary studies are high. As an important step forward, future studies that leverage
287 genomic data and fossil calibrations should consider comparing traditional phylogenetic clock
288 models and the MSC to evaluate the effects of ILS on divergence time estimation. We further
289 recommend that uncertainty in both mutation rates and generation times should be explicitly
290 incorporated in analyses wherein coalescent units are converted to absolute time [63, 72]. This
291 can be easily done by drawing mutation rates and generation times from prior distributions
292 rather than relying on point estimates, given that variation in inferred mutation rates can be high
293 among pedigrees [84], and mutation rates may change over time [27]. Moreover, estimating
294 generation times can be problematic, especially for perennial plants given the lack of clear
295 segregation in the germ line. The impact of the number, quality, and placement of fossil
296 calibrations – as well as model choice on divergence time estimation using traditional
297 phylogenetic concatenation methods – has been extensively studied [10, 38, 67, 69, 86].
298 Conversely, the careful evaluation of MSC methods for divergence time estimation is still in its
299 infancy. We therefore predict that future studies that directly compare the two approaches are
300 likely to identify as yet unrecognized though critical considerations for accurate divergence time
301 analysis.

302

303 **Concluding Remarks**

304 We conclude by noting that despite its advantages, the MSC method involves a heavy
305 computational burden and may not always be feasible for divergence time estimation on large
306 phylogenies [92-94]. In such cases, traditional phylogenetic clock analyses that use
307 concatenation may be the most practical approach [3, 30]. In particular, approximate likelihood
308 calculation appears useful in estimating divergence times for large phylogenies or for very long
309 alignments [86]. These models should not be seriously biased when divergence times are old

310 (Fig. 2) and ILS is low (Fig. 3). But given the prevalence of ILS across the tree of life, the
311 applications of the MSC for divergence time estimation in both shallow and **deep phylogenies**
312 will be of increasing interest and importance (see Outstanding Questions). It remains to be
313 seen to what degree divergence time estimates will agree when both traditional phylogenetic
314 clock models and mutation-rate calibrated MSC methods are applied within the same study
315 systems.

316

317 **Acknowledgements**

318 We thank Priya Moorjani for her helpful comments on an early version. The editor and two
319 anonymous reviewers provided comments that improved the manuscript. ADY gratefully
320 acknowledges the John Simon Guggenheim Foundation and the Alexander von Humboldt
321 Foundation for their support. ZY is supported by a Biotechnology and Biological Sciences
322 Research Council grant (BB/P006493/1).

323 **Glossary**

324 **Ancient DNA Methods:** Sequence data is obtained from the remains of ancient specimens.

325 The DNA is typically damaged and fragmented by absolute time and by exposure to damaging
326 agents such as heat, oxidation, and UV irradiation.

327 **Bayesian Methods:** Bayes theorem is used to approximate the maximum likelihood estimates
328 of a model and its parameters by sampling many estimates with proposal distributions and
329 commonly implemented with a Markov chain Monte Carlo algorithm. Prior distributions are used
330 to constrain the search space of parameters and may include *a priori* expectations for
331 parameter estimates but are often left vague. Bayesian methods are used as a matter of
332 computational convenience when maximum likelihood optimization is intractable.

333 **Callable Sites:** The number of sites where a *de novo* mutation should be detectable.

334 **Concatenation:** Multiple loci are treated as a single nonrecombining locus with a single
335 underlying topology.

336 **Coalescent:** The stochastic process of lineage joining when one traces the genealogical history
337 of a sample of sequences from a population backwards in time.

338 **Coalescent Age Estimate:** The divergence time for two sequences based on sampling theory
339 and measured in the expected number of generations.

340 **Coalescent Time Unit:** The expected coalescent time for a pair of sequences, which is $2N$
341 generations for a diploid species with population size N .

342 ***de novo* Mutation Rate:** The spontaneous germline mutation rate revealed in comparisons of
343 whole genomes from both parents and their progeny (aka, pedigree trios).

344 **Deep Phylogenies:** Phylogenies that contain species with high sequence divergence. In such
345 cases, substitutional saturation or "multiple hits," long-branch attraction, gene duplication and
346 loss, and model misspecification can result in gene tree discordance. ILS can still be a
347 substantial source of conflict between gene trees and species trees in deep phylogenies.

348 **Divergence Times:** The expected absolute age at which two species became isolated from
349 each other.

350 **Effective Population Size:** The number of individuals that would produce the observed rate of
351 genetic drift in an idealized Fisher-Wright population model.

352 **Fossil Calibrations:** Fossil evidence from morphological characters that can constrain the age
353 of the crown group of a clade (e.g., with a hard minimum and a soft maximum).

354 **Gene Flow:** Exchange of alleles between two populations.

355 **Gene Tree:** The evolutionary history of a short, nonrecombining segment of the genome

356 **Gene Tree Discordance:** Difference in gene tree topology from the species tree, possibly
357 caused by deep coalescence.

358 **Generation Time:** The average time between two generations which is often quantified as the
359 average age of parents at birth, averaged over individuals.

360 **Lineage sorting:** The process by which gene lineages become fixed within a species
361 such that all alleles within that species coalesce to a single ancestral allele within the
362 species lineage.

363 **Incomplete Lineage Sorting (ILS):** Failure for two sequences from two species to coalesce in
364 the most recent common ancestral species, also known as deep coalescence.

365 **Loci:** Orthologous non-recombining sequences. Each locus corresponds to an independent
366 gene tree.

367 **Markov chain Monte Carlo (MCMC):** a simulation approach for sampling from a target
368 distribution such as the posterior distribution of parameters in Bayesian inference.

369 **Molecular Clock:** Hypothesis that the rate of molecular evolution is constant over time and
370 among lineages.

371 **Most Recent Common Ancestor (MRCA):** The most recent node on a phylogeny from which
372 all individuals in a clade of interest are derived.

373 **Multispecies Coalescent (MSC):** The extension of the coalescent process to multiple species
374 which accommodates the species tree as well as the coalescent within populations.

375 **Pairwise Sequence Divergence:** The evolutionary distance between a pair of sequences
376 measured as the expected number of substitutions per site.

377 **Pedigree Trio:** A child and the two parents for whom whole genomes are sequenced and
378 compared to identify the new mutations in the child.

379 **Per-year Substitution Rates:** The number of substitutions per-site per-year that are obtained
380 when calibrating a phylogeny to absolute time with information at nodes or tips.

381 **Reciprocal Monophyly:** All alleles within a species coalesce with each other before the first
382 coalescence with an allele from another species.

383 **Relaxed Clock Models:** An extension of the strict clock model to allow changes in evolutionary
384 rate over branches in a phylogeny.

385 **Species Tree:** The evolutionary history of species, which is often estimated from many
386 individual gene trees or loci.

387 **Strict Molecular Clock:** A single rate of molecular evolution is enforced for all branches in a
388 phylogeny.

389 **Tip-Dating Methods:** Rates of molecular evolution are calibrated to absolute time by known
390 sampling dates of individuals, whether extant or extinct, at the tips of a phylogeny.

391 **Total-Evidence:** Morphological characters for extinct (fossil) and extant tips and rates of
392 morphological evolution are used to infer species divergence times jointly with molecular data.

393 **Traditional Phylogenetic Clock Models:** Models for divergence time estimation that assume
394 one tree and one set of divergence times for all loci.

395

396 **Box Legends**

397 **Box 1 – Incomplete Lineage Sorting on a Rooted Three-Taxon Species Tree.**

398 **Box 2 – Differences between Bayesian methods for divergence time estimation and**
399 **programs for implementing them.**

400

401 **Figure Legends**

402 **Figure 1 – Overview of the MSC model and its use for estimating absolute divergence**

403 **times with external mutation rate data.** *Input Data* – The MSC requires aligned orthologous

404 sequence data as input. There can be many individual loci, and each locus is assumed to be

405 non-recombining and not under selection. The MSC allows for multiple alleles per species per

406 locus, and sampling multiple alleles can improve parameter estimates. Although joint estimation

407 of the species tree and MSC parameters is possible, using a fixed species tree is

408 computationally more efficient. *Estimate MSC Parameters by MCMC* – The MSC estimates

409 model parameters with Bayesian **Markov chain Monte Carlo (MCMC)**. This requires a prior

410 distribution for all model parameters including population sizes (θ), species divergence times (τ),

411 and possibly rates among loci (r). The MSC estimates a gene tree for each locus ($1..n$) and the

412 coalescent times on those trees. Gene trees can be incongruent with the species tree. The

413 distribution of gene trees and their coalescent age estimates are used to jointly estimate θ and τ

414 on the species tree. *Calibrate with Mutation Rate* – A per-generation mutation rate (μ) is

415 obtained from independent pedigree-based studies and a generation time (g) is estimated from

416 the distribution of parent ages at the time of birth for offspring. μ and g can then be used to

417 obtain an absolute rate of evolution by multiplying τ by g/μ . μ can also be used to rearrange the

418 expression for θ and obtain absolute population sizes (N).

419

420 **Figure 2 – Overestimation of species divergence times from genetic distances.** a) Species
421 A and B diverged t_{AB} generations ago. Sequences A and B coalesced further back in time at t_{Seq}
422 generations ago, with a mean $t_{Seq} - t_{AB}$ of $2N_{AB}$ generations. b) Sequences were simulated under
423 the MSC for a pair of species with constant $N_{AB} = 10^5$ and $\mu = 1 \times 10^{-8}$ per site per generation. c)
424 The relative expected overestimation of species divergence times by $2N_{AB}$ becomes smaller as
425 t_{AB} becomes larger, because $2N_{AB}$ contributes only a small proportion of time to the overall
426 divergence time estimate.

427

428 **Figure 3 – Effects of ILS and the MSC on divergence time estimation.** Data are from Table
429 2 of Angelis and dos Reis [9]. a) Three-taxon species tree used for simulation. All data were
430 simulated under the MSC with the Jukes Cantor model of molecular evolution. A μ of 1×10^{-8}
431 per site per generation and a generation time of ten years was used, and the species tree root
432 (node r) had an age of 10 MYA or τ of 0.01. Data were simulated with 4 different population
433 sizes (N) that were constant along the species tree. The root was calibrated with a gamma
434 distribution as one might in a fossil-calibrated divergence time analysis. b) Divergence time
435 estimates of node s when using concatenation (MCMCTREE) or the MSC (BPP). Because the
436 calibration is placed on the older root node, the younger node is overestimated when N or ILS is
437 high by concatenation but not MSC methods. Points represent posterior means and error bars
438 are the 95% credible intervals.

439

440 **Figure 4 – Illustration of the consequences of differences between divergence time**
441 **estimates.** Pedigree symbols represent mutation rate-calibrated divergence times and
442 probability distributions represent traditional phylogenetic clock model estimates. a) The MRCA
443 of Madagascar's mouse lemurs. The mutation rate-calibrated MSC estimate yields a mean
444 divergence time of 1.5 MYA whereas a traditional phylogenetic clock model with fossil

445 calibrations recovers a divergence time estimate of approximately 10 Ma. Though the position of
446 Madagascar relative to Africa is essentially the same at these two geological time points,
447 Madagascar's climate would have been very similar to that of today at 1.5 MYA whereas it
448 would have been much warmer and drier 10 MYA. b) The divergence between Old World
449 monkeys and apes. A mutation rate-calibrated divergence time estimate (though not with the
450 MSC) is 62 MYA whereas the traditional phylogenetic clock model yields a divergence time
451 estimate of approximately 35 MYA. There are striking differences in both continental
452 configuration and climate between these two time points. At 62 MYA, the earth was largely
453 tropical and sea levels were markedly high, isolating Africa from the northern continents. At 35
454 MYA, Africa has shifted northward, making contact with the northern continents and Antarctica
455 is partially glaciated indicating much cooler global temperatures. Global maps provided courtesy
456 of the Deep Time Maps project.

- 457 1. Zuckerkandl, E. and Pauling, L. (1965) Molecules as documents of evolutionary history. *J*
458 *Theor Biol* 8 (2), 357-66.
459
- 460 2. Thorne, J.L. et al. (1998) Estimating the rate of evolution of the rate of evolution. *MBE* 15
461 (12), 1647-1657.
462
- 463 3. Drummond, A.J. et al. (2006) Relaxed phylogenetics and dating with confidence. *PLoS Biol* 4
464 (5), e88.
465
- 466 4. dos Reis, M. et al. (2016) Bayesian molecular clock dating of species divergences in the
467 genomics era. *Nat Rev Genet* 17 (2), 71-80.
468
- 469 5. Rannala, B. and Yang, Z. (2003) Bayes estimation of species divergence times and ancestral
470 population sizes using DNA sequences from multiple loci. *Genetics* 164, 1645-1656.
471
- 472 6. Ogilvie, H.A. et al. (2017) StarBEAST2 Brings Faster Species Tree Inference and Accurate
473 Estimates of Substitution Rates. *Mol Biol Evol* 34 (8), 2101-2114.
474
- 475 7. Stange, M. et al. (2018) Bayesian divergence-time estimation with genome-wide single-
476 nucleotide polymorphism data of sea catfishes (Ariidae) supports Miocene closure of the
477 Panamanian Isthmus. *Syst Biol* 67 (4), 681-699.
478
- 479 8. Burgess, R. and Yang, Z. (2008) Estimation of hominoid ancestral population sizes under
480 bayesian coalescent models incorporating mutation rate variation and sequencing errors. *Mol*
481 *Biol Evol* 25 (9), 1979-94.
482
- 483 9. Angelis, K. and dos Reis, M. (2015) The impact of ancestral population size and incomplete
484 lineage sorting on Bayesian estimation of species divergence times. *Current Zoology* 61 (5),
485 874–885.
486
- 487 10. Liu, L. et al. (2017) Genomic evidence reveals a radiation of placental mammals
488 uninterrupted by the KPg boundary. *Proc Natl Acad Sci U S A* 114 (35), E7282-E7290.
489
- 490 11. Hackel, J. et al. (2018) Grass diversification in Madagascar: In situ radiation of two large C3
491 shade clades and support for a Miocene to Pliocene origin of C4 grassy biomes. *Journal of*
492 *Biogeography* 45 (4), 750-761.
493
- 494 12. Kawahara, A.Y. et al. (2019) Phylogenomics reveals the evolutionary timing and pattern of
495 butterflies and moths. *Proc Natl Acad Sci U S A* 116 (45), 22657-22663.
496
- 497 13. Betts, H.C. et al. (2018) Integrated genomic and fossil evidence illuminates life's early
498 evolution and eukaryote origin. *Nat Ecol Evol* 2 (10), 1556-1562.
499
- 500 14. Benton, M.J. and Donoghue, P.C. (2007) Paleontological evidence to date the tree of life.
501 *Mol Biol Evol* 24 (1), 26-53.
502
- 503 15. De Baets, K. et al. (2016) Tectonic blocks and molecular clocks. *Philos Trans R Soc Lond B*
504 *Biol Sci* 371 (1699).
505
- 506 16. Rannala, B. (2016) Conceptual issues in Bayesian divergence time estimation. *Philos Trans*
507 *R Soc Lond B Biol Sci* 371 (1699).

- 508
509 17. Wing, S.L. et al. (2009) Late Paleocene fossils from the Cerrejon Formation, Colombia, are
510 the earliest record of Neotropical rainforest. *Proc Natl Acad Sci U S A* 106 (44), 18627-32.
511
512 18. Bloch, J.I. et al. (2016) First North American fossil monkey and early Miocene tropical biotic
513 interchange. *Nature* 533 (7602), 243-6.
514
515 19. Kidwell, S.M. (2001) Major biases in the fossil record. In *Paleobiology II* (Briggs, D.E.G. and
516 Crowther, P.R. eds), pp. 297-303, Blackwell Science Ltd.
517
518 20. Kergoat, G.J. et al. (2018) Opposite macroevolutionary responses to environmental changes
519 in grasses and insects during the Neogene grassland expansion. *Nat Commun* 9 (1), 5089.
520
521 21. Castroviejo-Fisher, S. et al. (2014) Neotropical diversification seen through glassfrogs.
522 *Journal of Biogeography* 41 (1), 66-80.
523
524 22. Langley, C.H. and Fitch, W.M. (1974) An examination of the constancy of the rate of
525 molecular evolution. *JME* 3, 161-177.
526
527 23. Lynch, M. et al. (2016) Genetic drift, selection and the evolution of the mutation rate. *Nat*
528 *Rev Genet* 17 (11), 704-714.
529
530 24. Li, W.-H. et al. (1996) Rates of nucleotide substitution in primates and rodents and the
531 generation-time effect hypothesis. *Molecular Phylogenetics and Evolution* 5 (1), 182-187.
532
533 25. Mello, B. and Schrago, C.G. (2019) The estimated pacemaker for great apes supports the
534 hominoid slowdown hypothesis. *Evolutionary Bioinformatics* 15, 1-8.
535
536 26. Goodman, M. (1985) Rates of molecular evolution: the hominoid slowdown. *Bioessays* 3 (1),
537 9-14.
538
539 27. Moorjani, P. et al. (2016) Variation in the molecular clock of primates. *Proc Natl Acad Sci U*
540 *S A* 113 (38), 10607-12.
541
542 28. Smith, S.A. and Donoghue, M.J. (2008) Rates of molecular evolution are linked to life history
543 in flowering plants. *Science* 322 (5898), 86-9.
544
545 29. Lanfear, R. et al. (2013) Taller plants have lower rates of molecular evolution. *Nat Commun*
546 4, 1879.
547
548 30. Rannala, B. and Yang, Z.H. (2007) Inferring speciation times under an episodic molecular
549 clock. *Systematic Biology* 56 (3), 453-466.
550
551 31. Ho, S.Y. and Duchene, S. (2014) Molecular-clock methods for estimating evolutionary rates
552 and timescales. *Mol Ecol* 23 (24), 5947-65.
553
554 32. Yoder, A.D. and Yang, Z.H. (2000) Estimation of primate speciation dates using local
555 molecular clocks. *MBE* 17 (7), 1081-1090.
556
557 33. Sanderson, M.J. (1997) A nonparametric approach to estimating divergence times in the
558 absence of rate constancy. *MBE* 14 (12), 1218-1231.

559
560 34. Sanderson, M.J. (2002) Estimating absolute rates of molecular evolution and divergence
561 times: a penalized likelihood approach. *MBE* 19 (1), 101-109.
562
563 35. Huelsenbeck, J.P. et al. (2000) A Compound Poisson Process for Relaxing the Molecular
564 Clock. *Genetics* 154, 1879-1892.
565
566 36. Lepage, T. et al. (2007) A general comparison of relaxed molecular clock models. *Mol Biol*
567 *Evol* 24 (12), 2669-80.
568
569 37. Lartillot, N. et al. (2016) A mixed relaxed clock model. *Philos Trans R Soc Lond B Biol Sci*
570 371 (1699).
571
572 38. Warnock, R.C. et al. (2015) Calibration uncertainty in molecular dating analyses: there is no
573 substitute for the prior evaluation of time priors. *Proc Biol Sci* 282 (1798), 20141013.
574
575 39. Parham, J.F. et al. (2012) Best practices for justifying fossil calibrations. *Syst Biol* 61 (2),
576 346-59.
577
578 40. Heath, T.A. et al. (2014) The fossilized birth-death process for coherent calibration of
579 divergence-time estimates. *Proc Natl Acad Sci U S A* 111 (29), E2957-66.
580
581 41. Ronquist, F. et al. (2012) A total-evidence approach to dating with fossils, applied to the
582 early radiation of the hymenoptera. *Syst Biol* 61 (6), 973-99.
583
584 42. Zhang, C. et al. (2016) Total-Evidence Dating under the Fossilized Birth-Death Process.
585 *Syst Biol* 65 (2), 228-49.
586
587 43. Gavryushkina, A. et al. (2017) Bayesian Total-Evidence Dating Reveals the Recent Crown
588 Radiation of Penguins. *Syst Biol* 66 (1), 57-73.
589
590 44. Alvarez-Carretero, S. et al. (2019) Bayesian Estimation of Species Divergence Times Using
591 Correlated Quantitative Characters. *Syst Biol* 68 (6), 967-986.
592
593 45. Silvestro, D. et al. (2018) Closing the gap between palaeontological and neontological
594 speciation and extinction rate estimates. *Nat Commun* 9 (1), 5237.
595
596 46. Rambaut, A. (2000) Estimating the rate of molecular evolution: incorporating non-
597 contemporaneous sequences into maximum likelihood phylogenies. *Bioinformatics* 16 (4), 395-
598 399.
599
600 47. Stadler, T. and Yang, Z.H. (2013) Dating phylogenies with sequentially sampled tips.
601 *Systematic Biology* 62 (5), 674-688.
602
603 48. Worobey, M. et al. (2008) Direct evidence of extensive diversity of HIV-1 in Kinshasa by
604 1960. *Nature* 455 (7213), 661-4.
605
606 49. Chang, D. et al. (2017) The evolutionary and phylogeographic history of woolly mammoths:
607 a comprehensive mitogenomic analysis. *Sci Rep* 7, 44585.
608

- 609 50. Llamas, B. and al., e. (2016) Ancient mitochondrial DNA provides high-resolution time scale
610 of the peopling of the Americas. *Sci. Adv.*
611
- 612 51. Orlando, L. et al. (2013) Recalibrating Equus evolution using the genome sequence of an
613 early Middle Pleistocene horse. *Nature* 499 (7456), 74-8.
614
- 615 52. Kingman, J.F.C. (1982) The coalescent. *Stochastic Processes and their Applications* 13,
616 235-248.
617
- 618 53. Xu, B. and Yang, Z. (2016) Challenges in Species Tree Estimation Under the Multispecies
619 Coalescent Model. *Genetics* 204 (4), 1353-1368.
620
- 621 54. Rannala, B. et al. (2020) The multispecies coalescent model and species tree inference. In
622 *Phylogenetics in the Genomic Era* (Scoenavacca, C. et al. eds), pp. 1-20.
623
- 624 55. Maddison, W.P. (1997) Gene Trees in Species Trees. *Syst Biol* 46 (3), 523-536.
625
- 626 56. Rokas, A. et al. (2003) Genome-scale approaches to resolving incongruence in molecular
627 phylogenies. *Nature* 425, 798-804.
628
- 629 57. Yang, Z. (2014) *Molecular Evolution: A Statistical Approach*, Oxford University Press.
630
- 631 58. Flouri, T. et al. (2020) A Bayesian Implementation of the Multispecies Coalescent Model
632 with Introgression for Phylogenomic Analysis. *Mol Biol Evol* 37 (4), 1211-1223.
633
- 634 59. Edwards, S.V. and Beerli, P. (2000) Perspective: gene divergence, population divergence,
635 and the variance in coalescence time in phylogeographic studies. *Evolution* 54 (6), 1839-1854.
636
- 637 60. Carstens, B.C. and Knowles, L.L. (2007) Estimating species phylogeny from gene-tree
638 probabilities despite incomplete lineage sorting: An example from *Melanoplus* grasshoppers.
639 *Systematic Biology* 56 (3), 400-411.
640
- 641 61. Mendes, F.K. and Hahn, M.W. (2016) Gene Tree Discordance Causes Apparent
642 Substitution Rate Variation. *Syst Biol* 65 (4), 711-21.
643
- 644 62. Fang, B. et al. (2020) Estimating uncertainty in divergence times among three-spined
645 stickleback clades using the multispecies coalescent. *Mol Phylogenet Evol* 142, 106646.
646
- 647 63. Schüßler, D. et al. (2019) Cryptic patterns of speciation in cryptic primates: microendemic
648 mouse lemurs and the multispecies coalescent. *bioRxiv*.
649
- 650 64. Liu, W. et al. (2019) An evolutionarily stable strategy to colonize spatially extended habitats.
651 *Nature* 575 (7784), 664-668.
652
- 653 65. Oliveros, C.H. et al. (2019) Earth history and the passerine superradiation. *Proc Natl Acad*
654 *Sci U S A* 116 (16), 7916-7925.
655
- 656 66. Li, H.T. et al. (2019) Origin of angiosperms and the puzzle of the Jurassic gap. *Nat Plants* 5
657 (5), 461-470.
658

- 659 67. Barba-Montoya, J. et al. (2018) Constraining uncertainty in the timescale of angiosperm
660 evolution and the veracity of a Cretaceous Terrestrial Revolution. *New Phytol* 218 (2), 819-834.
661
- 662 68. Beaulieu, J.M. et al. (2015) Heterogeneous Rates of Molecular Evolution and Diversification
663 Could Explain the Triassic Age Estimate for Angiosperms. *Syst Biol* 64 (5), 869-78.
664
- 665 69. Magallon, S. et al. (2015) A metacalibrated time-tree documents the early rise of flowering
666 plant phylogenetic diversity. *New Phytol* 207 (2), 437-453.
667
- 668 70. Leebens-Mack and One Thousand Plant Transcriptomes, I. (2019) One thousand plant
669 transcriptomes and the phylogenomics of green plants. *Nature* 574 (7780), 679-685.
670
- 671 71. Flouri, T. et al. (2018) Species Tree Inference with BPP Using Genomic Sequences and the
672 Multispecies Coalescent. *Mol Biol Evol* 35 (10), 2585-2593.
673
- 674 72. Yoder, A.D. et al. (2016) Geogenetic patterns in mouse lemurs (genus *Microcebus*) reveal
675 the ghosts of Madagascar's forests past. *Proc Natl Acad Sci U S A* 113 (29), 8049-56.
676
- 677 73. Federman, S. et al. (2018) Reconciling species diversity in a tropical plant clade (*Canarium*,
678 *Burseraceae*). *PLoS One* 13 (6), e0198882.
679
- 680 74. Keightley, P.D. et al. (2015) Estimation of the spontaneous mutation rate in *Heliconius*
681 *melpomene*. *Mol Biol Evol* 32 (1), 239-43.
682
- 683 75. Smeds, L. et al. (2016) Direct estimate of the rate of germline mutation in a bird. *Genome*
684 *Res* 26 (9), 1211-8.
685
- 686 76. Pfeifer, S.P. (2017) Direct estimate of the spontaneous germ line mutation rate in African
687 green monkeys. *Evolution* 71 (12), 2858-2870.
688
- 689 77. Thomas, G.W.C. et al. (2018) Reproductive longevity predicts mutation rates in primates.
690 *Curr Biol* 28 (19), 3193-3197 e5.
691
- 692 78. Koch, E. et al. (2019) De novo mutation rate estimation in wolves of known pedigree. *Mol*
693 *Biol Evol*.
694
- 695 79. Wang, L. et al. (2019) The architecture of intra-organism mutation rate variation in plants.
696 *PLoS Biol* 17 (4), e3000191.
697
- 698 80. Pierron, D. et al. (2017) Genomic landscape of human diversity across Madagascar. *Proc*
699 *Natl Acad Sci U S A* 114 (32), E6498-E6506.
700
- 701 81. Lawal, R.A. et al. (2020) The wild species genome ancestry of domestic chickens. *BMC Biol*
702 18 (1), 13.
703
- 704 82. Smith, O. et al. (2019) A domestication history of dynamic adaptation and genomic
705 deterioration in *Sorghum*. *Nat Plants* 5 (4), 369-379.
706
- 707 83. Wu, D.D. et al. (2018) Pervasive introgression facilitated domestication and adaptation in
708 the *Bos* species complex. *Nat Ecol Evol* 2 (7), 1139-1145.
709

710 84. Smith, T.C.A. et al. (2018) Large scale variation in the rate of germ-line de novo mutation,
711 base composition, divergence and diversity in humans. *PLoS Genet* 14 (3), e1007254.
712

713 85. Lewin, H.A. et al. (2018) Earth BioGenome Project: Sequencing life for the future of life.
714 *Proc Natl Acad Sci U S A* 115 (17), 4325-4333.
715

716 86. dos Reis, M. et al. (2018) Using Phylogenomic Data to Explore the Effects of Relaxed
717 Clocks and Calibration Strategies on Divergence Time Estimation: Primates as a Test Case.
718 *Syst Biol* 67 (4), 594-615.
719

720 87. Moorjani, P. et al. (2016) Human Germline Mutation and the Erratic Evolutionary Clock.
721 *PLoS Biol* 14 (10), e2000744.
722

723 88. Scally, A. et al. (2012) Insights into hominid evolution from the gorilla genome sequence.
724 *Nature* 483 (7388), 169-75.
725

726 89. Ho, S.Y. et al. (2011) Bayesian estimation of substitution rates from ancient DNA sequences
727 with low information content. *Syst Biol* 60 (3), 366-75.
728

729 90. Exposito-Alonso, M. et al. (2018) The rate and potential relevance of new mutations in a
730 colonizing plant lineage. *PLoS Genet* 14 (2), e1007155.
731

732 91. Yang, Z.H. and Yoder, A.D. (2003) Comparison of likelihood and Bayesian methods for
733 estimating divergence times using multiple gene loci and calibration points, with application to a
734 radiation of cute-looking mouse lemur species. *Systematic Biology* 52 (5), 705-716.
735

736 92. Campbell, C.R. et al. (2019) Pedigree-based measurement of the de novo mutation rate in
737 the gray mouse lemur reveals a high mutation rate, few mutations in CpG sites, and a weak sex
738 bias. *bioRxiv*.
739

740 93. Zanne, A.E. et al. (2014) Three keys to the radiation of angiosperms into freezing
741 environments. *Nature* 506 (7486), 89-92.
742

743 94. Jetz, W. et al. (2012) The global diversity of birds in space and time. *Nature* 491 (7424),
744 444-8.
745

746 95. Hudson, R.R. (1983) Testing the constant-rate neutral allele model with protein sequence
747 data. *Evolution* 37 (1), 203-217.
748

749 96. Bouckaert, R. et al. (2019) BEAST 2.5: An advanced software platform for Bayesian
750 evolutionary analysis. *PLoS Computational Biology* 15 (4), e1006650.
751

752 97. Yang, Z. (2007) PAML 4: phylogenetic analysis by maximum likelihood. *Mol Biol Evol*, 24
753 (8), 1586–1591.
754

755 98. Ronquist F. et al. (2012) MrBayes 3.2: Efficient Bayesian phylogenetic inference and model
756 choice across a large model space. *Systematic Biology* 61 (3), 539-542.
757

758 99. Lartillot, N. and Philippe, H. A. (2004) A Bayesian mixture model for across-site
759 heterogeneities in the amino acid replacement process. *Mol Biol Evol*, 21 (6), 1095-1109.
760

Highlights

- Molecular clock models using fossil calibrations have allowed investigators to estimate the age of speciation events.
- Theoretical and computational developments have relaxed the assumption of a molecular clock, thus improving the accuracy of divergence time estimation.
- Despite these advances, estimates can be biased when there is widespread incomplete lineage sorting (ILS).
- Increased understanding of gene tree heterogeneity has driven multispecies coalescent (MSC) methods to prominence, though the potential power of the MSC for divergence time estimation remains largely unexplored.
- Absolute times can be obtained by using mutation rates estimated from pedigrees, providing [some] freedom from the incomplete fossil record.
- Mutation-rate calibrated MSC methods and traditional phylogenetic clock-dating methods with fossil calibrations can yield strikingly different divergence times.

Outstanding Questions

- To what extent is among-lineage rate variation modeled by relaxed clock methods due to gene tree discordance from ILS?
- Have divergence times throughout the tree of life been systematically overestimated in clades that rely on external, and typically older, calibrations?
- Do divergence time estimates based on per-generation mutation rates and per-year substitution rates yield similar results, especially if substitution rates are estimated from presumably neutral regions of the genome such as third codon positions?
- Will MSC estimates that leverage fossil calibrations bring new insights to contentious age estimates such as the origins of placental mammals or angiosperms?
- Should effective population size variation among species be a concern for divergence time estimation studies using concatenation?
- Can mutation-rate calibrated MSC methods that account for variable rates and generation times among branches improve divergence time estimation for clades that have rapid life history transitions?
- How can we develop standard operating procedures for evaluating the strength of evidence for divergence time estimates from traditional phylogenetic analyses versus ages inferred from MSC methods that rely on mutation rate and generation time estimates?
- Are there alternative ways forward for estimating the absolute age of clades with poor or non-existent fossil representation?
- To what extent do the methods (MSC versus concatenation) and the calibrations (mutation rate versus fossils) impact divergence time estimates?

Key Figure Data

Estimate MSC Parameter with MCMC Calibration and Mutation Rate

Click MCMC access Calibration and Mutation Rate
[Figure; Fig1.pdf](#)

Aligned Sequences

A1	GTTATGGACTTA
A2	GTTATGGATTTA
B1	GATAAGGAGTTA
B2	GATAAGGAGTTA
C1	GAGAAGGAGT-A
C2	GAGAAGGAGT-A

1 2 n

Individual Map

Allele Species

A1	A
A2	A
B1	B
B2	B
C1	C
C2	C

Species Topology

Prior Distributions

$\theta \sim \text{inv}\Gamma(\alpha, \beta)$

θ τ r

Gene Tree Posterior Distributions

1 2 n

Mutation Rate Estimation

μ

Generation Time Estimation

g

MSC Parameter Posterior Distributions

A B C

Absolute Divergence Time

$\tau = \mu t$ (MSC branch lengths)
 t (number of generations)
 μ (mutations per site per generation)
 g (number of years per generation)

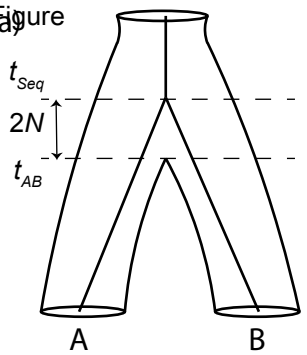
Absolute Time = $\frac{\tau g}{\mu} = tg$

Absolute Population Size

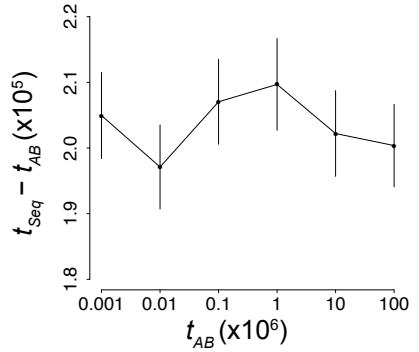
$\theta = 4N\mu$ (MSC ancestral population size)

Absolute Size = $\frac{\theta}{4\mu} = N$

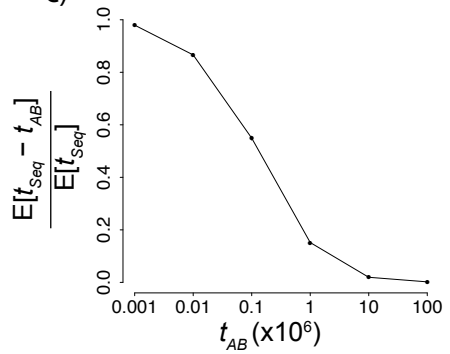
Figure

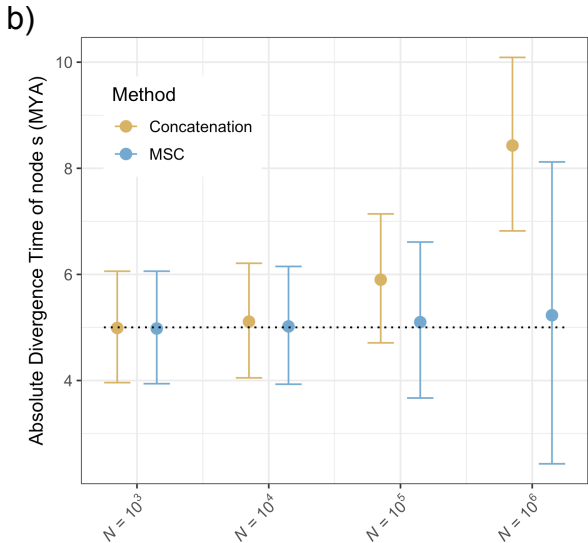
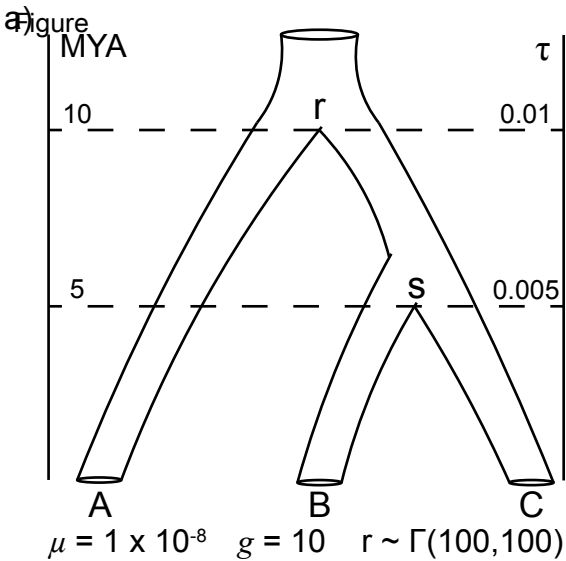


b)



c)





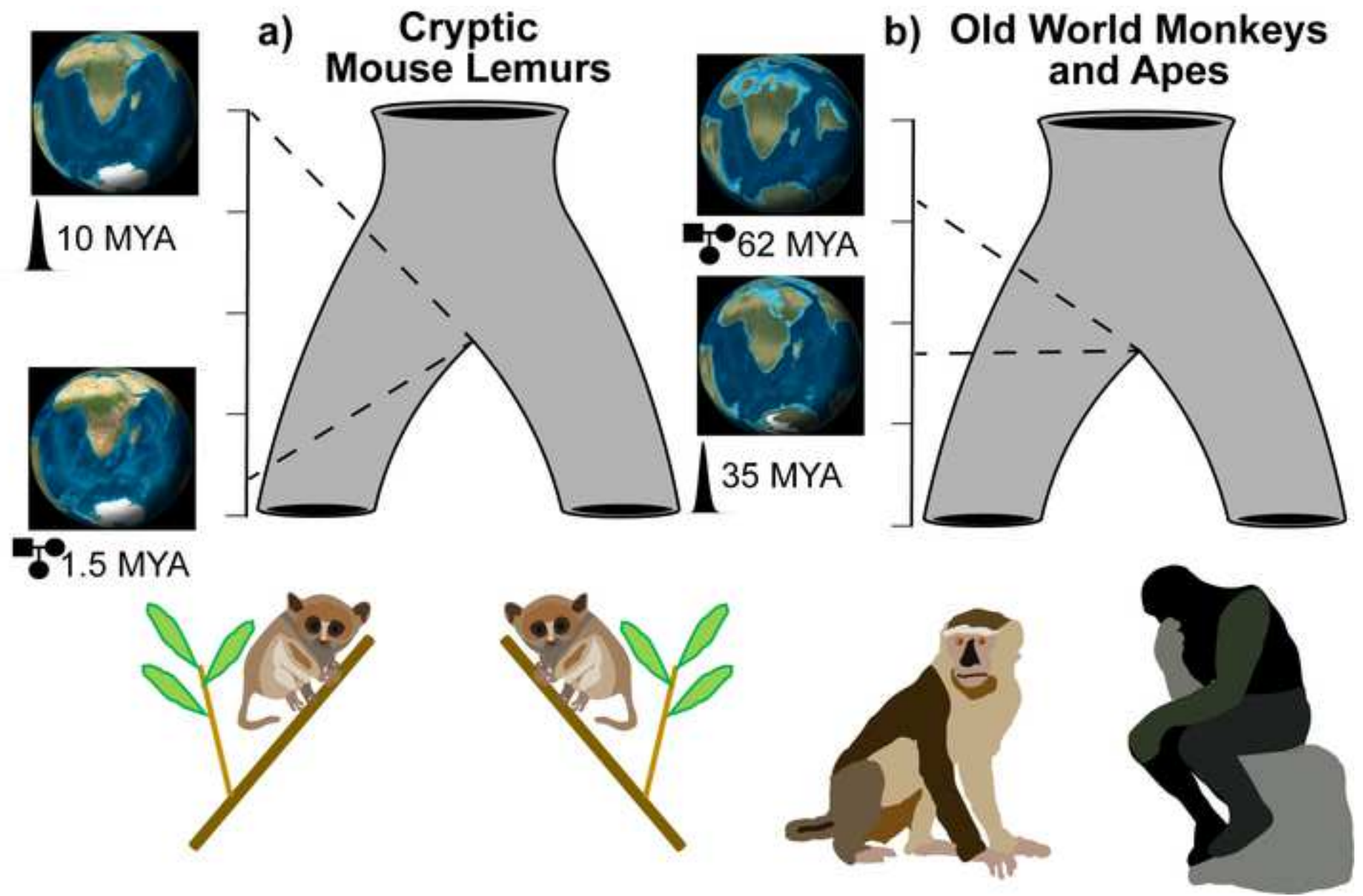
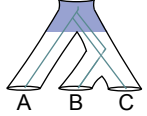
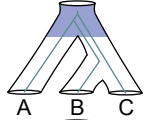
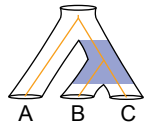
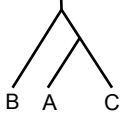
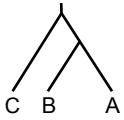
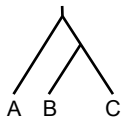
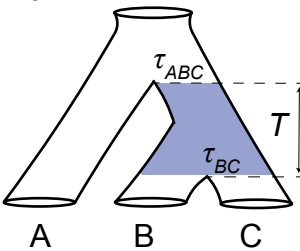


Figure Species Tree

Gene Tree

Embedded Gene Tree

Probability



$$1 - (2/3)e^{-T}$$

$$(1/3)e^{-T}$$

$$(1/3)e^{-T}$$

ILS occurs when B and C do not coalesce within T , the time between τ_{BC} and τ_{ABC} measured in $2N_{BC}$ generations. ILS can be identified visually by embedding gene trees within the species tree. The neutral coalescent provides expectations for the frequency with which ILS occurs that are dependent on T alone [95]. When T is 0, 2/3 of gene trees are expected not to match the species tree due to ILS. Less than 1% of gene trees are expected to be discordant around T of 5. The absolute divergence time does not affect T .

Probability of a Discordant Gene Tree = $(2/3) e^{-T}$

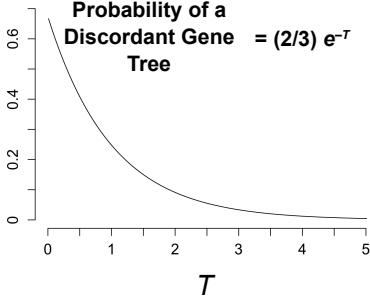
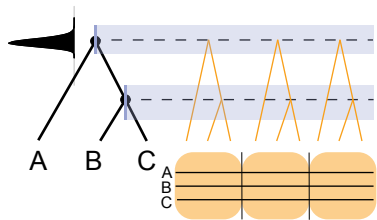
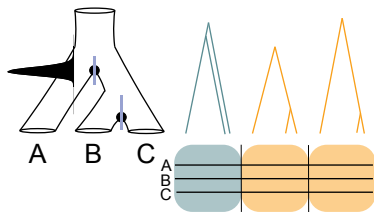


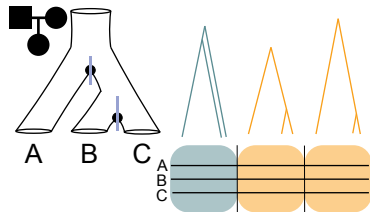
Figure Concatenation with Fossil Calibrations



MSC with Fossil Calibrations



Mutation Rate Calibrated MSC



Strengths

Computationally efficient for large numbers of tips and loci

Considers discordance between gene trees and species trees

Does not require calibrations on nodes from external information such as fossils

Weaknesses

May produce biased estimates when ILS is high or when gene sequence divergence is far from species divergence

Increased computational complexity from averaging over gene trees to estimate species tree parameters

Requires external mutation rate estimates from sequenced pedigrees and potentially not appropriate for distant taxa

Common Programs

BEAST2 [96]
MCMCTREE [97]
MrBayes [98]
PhyloBayes [99]

BPP [5,71]
StarBEAST2 [6]

BPP [5,71]
StarBEAST2 [6]